TOPS DIFFERENTIAL SAR INTERFEROMETRY WITH TERRASAR-X

Luca Marotti[(1)], Pau Prats[(1)], Rolf Scheiber[(1)], Steffen Wollstadt[(1)], Andreas Reigber[(1)]

[(1)]German Aerospace Center (DLR),Microwave and Radar Institute, Oberpfaffenhofen,82234 Wessling, Germany.
Email: luca.marotti@dlr.de

ABSTRACT

In this paper we investigate the possibility to exploit TOPS data to measure ground displacement movements by means of Differential SAR Interferometry (DInSAR). Several critical points (i.e. coregistration) have to be faced during the data processing since, due to the TOPS signal characteristics, the interferometric chain is very sensitive to small implementation errors. The obtained results will be compared with the ones conventionally retrieved when applying DInSAR on stripmap data. Finally, the potential of DInSAR measurements, when combining TOPS and stripmap data by means of point-like scatterers, will be also analyzed. The work presented in this study was funded under ESA-ESTEC contract number 22243/09/NL/JA.

1. INTRODUCTION

Differential SAR Interferometry (DInSAR) is a remote sensing technique that allows the investigation of the deformation phenomena occurring on the Earth surface. Basically, DInSAR is based on the capability of a radar to accurately measure the range distance, which allows the retrieval of the surface movements of the observed scene with an accuracy ranging from few centimeters to millimeters. Since its introduction DInSAR has been successfully exploited for the generation of large scale deformations maps. Moreover, if several SAR images of the test area are available, the technique permits to monitor the temporal evolution of the detected displacement by exploiting the interferometric phases of the data stack [1]-[3].

Conventionally, DInSAR investigations have been performed on data acquired in stripmap mode. Clearly a wider coverage of the investigated area might be an advantage for seismology, subsidence monitoring and civil protection purposes. For these reasons, in this paper, we perform the analysis of the DInSAR technique by means of data acquired in TOPS mode [4]. Note that TOPS will be the default mode of ESA's Sentinel-1 (S-1) satellite. In this mode the acquisition is performed steering the antenna in the along track direction from backward to forward. At the end of the burst the antenna look angle is changed to illuminate a second subswath, pointing again backward. When the last subswath is imaged, the antenna points back to the first subswath, so that no gaps are left between bursts of the same subswath. The fast steering leads to a reduction of the observation time and, consequently, to a worsening of the azimuth resolution. However all targets are observed by a complete antenna pattern and, therefore, it is possible to overcomes the problems of scalloping and azimuth varying signal-to-noise ratio of the conventional ScanSAR mode.

One of the most challenging aspects in TOPS Interferometry is the fact that the acquired signal has an azimuth varying Doppler centroid. Such a variation increases the requirements in term of coregistration accuracy [5]. Therefore in this study, we will perform the precise coregistration of the data stack following a two step approach. In the first step the data are geometrically coregistered with the use of an external Digital Elevation Model (DEM) and the orbit information. In the second step, the residual misregistration is estimated trough the spectral diversity (SD) technique.

Finally, DInSAR results obtainable by the generation of cross interferograms between TOPS and stripmap data will be also addressed. This combination might be of interest for several reasons. On the one hand, when using TOPS mode, it would be possible not to break the data continuity of data acquired in stripmap mode by previous sensors. On the other hand, the use of two different modes over the same area at different time instants might be of interest due to different applications or user needs. Due to the different acquisition modes, only a part of the azimuth frequencies of the signal spectra acquired in TOPS mode will overlap with the one acquired in stripmap mode. For this reason, for distributed targets, a cross-interferogram will result totally decorrelated at the burst edges. Therefore, the exploitation of such interferograms will be performed by means of Coherent Scatterers (CS) [6]. Such scatterers, indeed, are characterized by a completely correlated object spectrum. Therefore they will remain coherent also when combining different spectral sub-bands of the acquired signals.

2. TOPS AND STRIPMAP DINSAR

2.1. Processing Chain

In order to retrieve the temporal evolution of the deformation, a simple version of the so called small baseline technique (SBAS) [3] has been used for the DInSAR processing chain (Fig. 1).

After accurate coregistration, all the interferograms obtained with respect to a common master have been generated. Then the SRTM phases have been removed from each interferogram and a multilook window of size 30m x 30m has been applied for noise reduction. The same window size has been also used for the estimation of the coherence. The pixels with a mean interferometric coherence, computed over all 7 interferograms, grater than 0.6 have been selected for the DInSAR processing. The resulting residual phases have been unwrapped and calibrated with a reference point (the Azteca Stadium). Then, a least-square (LS) approach has been used to estimate the residual DEM errors and low pass (LP) deformation, i.e.: the mean deformation velocity. After subtracting these two components, the atmospheric phase screen (APS) has been estimated by performing in cascade a low pass filter (LP) in the space domain (about 1km x 1km size) and a high pass filter (HP) in the time domain. Afterwards the APS is removed for each interferogram and the LP temporal component is reinstated. The obtained filtered data correspond to the temporal evolution of the deformation.

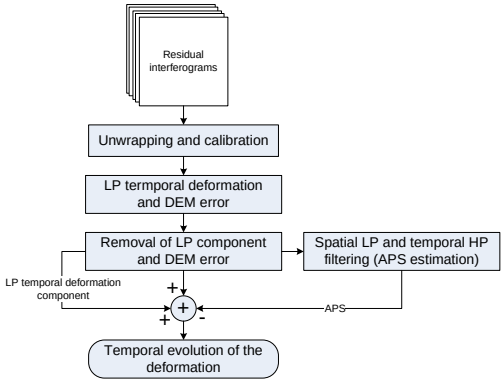

Figure 1. DInSAR processing chain.

2.2. DInSAR Experimental Results

The above described processing chain has been applied to both TOPS and stripmap image stacks. Those stacks are constituted by 8 TOPS images, acquired between September 20th 2009 and February 21st 2010, and 8 stripmap images, acquired between October 1st 2009 and March 4th 2010. Both data sets cover a time span of about 5 months and have an interleaving time of 11 days with respect to each other, i.e., 22 days between images acquired with the same mode. The data have been acquired over Mexico City, which is suffering of a severe subsidence due to ground water extraction.

The processing has been applied to both TOPS and stripmap image stacks. Fig. 2 shows the estimated mean deformation velocity overlaid over Google Earth, which appears similar in both cases (in the case of TOPS only the corresponding stripmap swath is shown). Note that the stripmap results look more stable and with less artifacts. This is due to the more uniform distribution of the baselines (Fig. 3), which favors the removal of DEM errors as well as facilitates the estimation of the mean deformation velocity.

The temporal evolution, for both TOPS and stripmap, of four points of interests inside the city area is shown in Fig. 4 and Fig. 5 respectively. For those plots it can be inferred that the TOPS results are slightly overestimated mainly due to the homogeneity of the baselines.

In any case it is possible to note that, in none of the shown results, any effects are visible at burst edges due to the higher Doppler centroids. The lack of phase artifacts at burst edges occurs thanks to the accurate azimuth coregistration performed.

3. TOPS STRIPMAP CROSS-INTERFEROGRAMS

3.1. Rationale

Fig. 6 plots the time-frequency diagrams for TOPS and stripmap in the case of full resolution stripmap (left) and in the case the stripmap signal has been filtered to the same resolution as TOPS (right). The diagonal grey strips represent the signal spectrum of two consecutive TOPS bursts, while the blue strip represents the stripmap signal spectrum. The darker areas correspond to the overlapping part of the spectra. Looking at those time-frequency diagrams, it is clear that a cross-interferogram will result in total decorrelation at burst edges. Fig. 7 exemplifies this fact by showing the result of a cross-interferogram with real TerraSAR-X data with the first images acquired over Mexico City with TOPS and stripmap in the descending configuration. The third sub-swath was selected for the TOPS case, since it corresponds to the stripmap swath. As expected, in the middle of the burst there is spectral correlation and therefore the coherence and the phase have useful information over distributed scatterers. However, as the spectral decorrelation decreases to zero, the coherence begins to decrease also, and the phase appears completely noisy.

After observing these results, it is clear that the exploitation of TOPS-stripmap cross-interferograms is

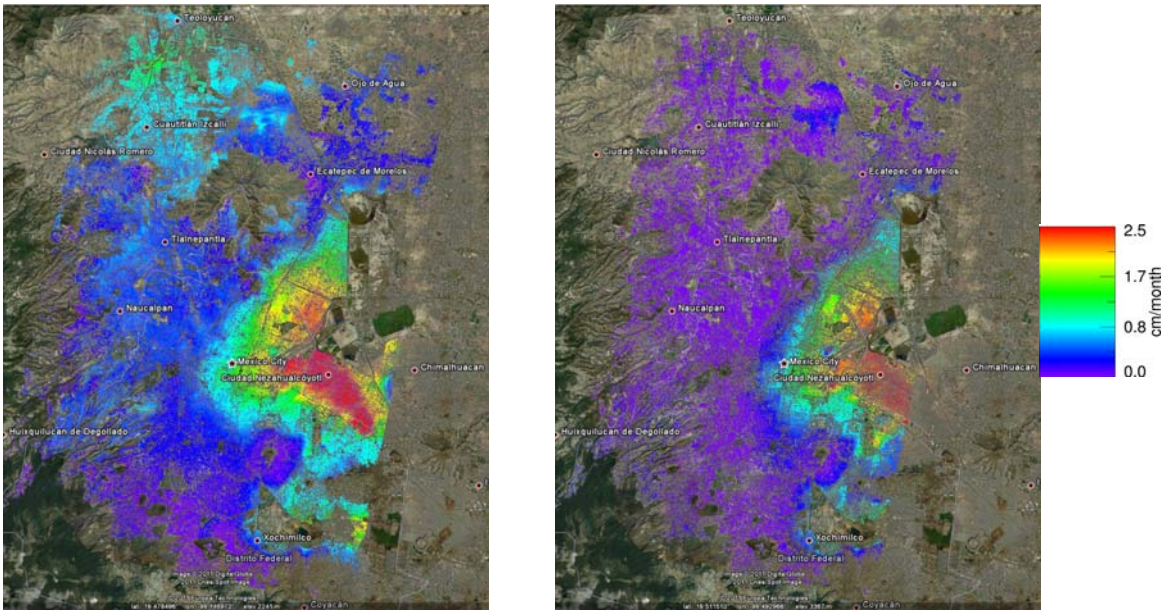

Figure 2. Obtained mean deformation velocities for TOPS (left) and stripmap (right).

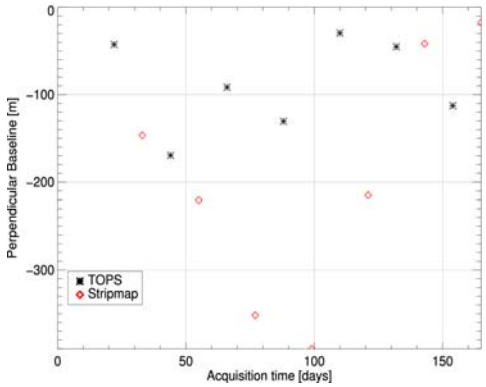

Figure 3. Perpendicular baseline distribution for the TOPS and stripmap dataset.

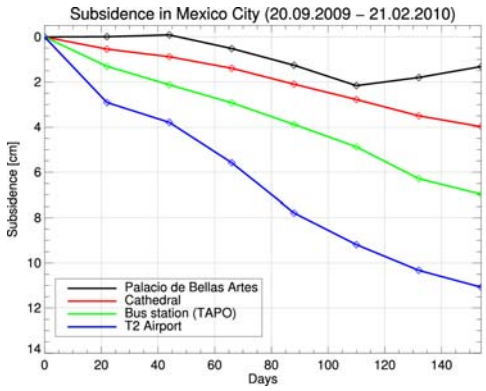

Figure 4. Temporal evolution of the deformation for four points of interests in Mexico City: TOPS data case.

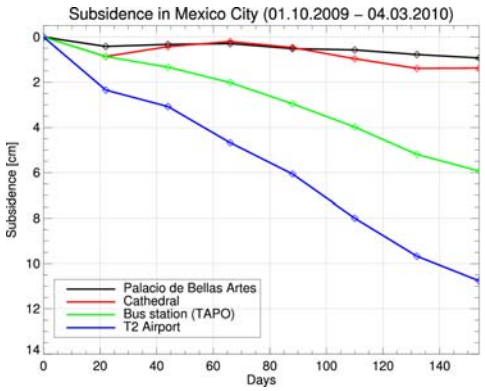

Figure 5. Temporal evolution of the deformation for four points of interests in Mexico City: stripmap data case.

only viable if the targets behave as an ideal point-like scatterer. Due to the lack of images series, the cross-interferogram analysis results, presented in the next section, have been obtained detecting point-like scatterers with the CS technique. Such targets, by definition, will have correlation between independent spectral looks, either in the range or the azimuth dimension.

3.2. Experimental Results

The combination of TOPS and stripmap data by means of CS has been investigated performing the cross-interferograms between one burst of the TOPS data and the corresponding patch in the stripmap data. It is worth to remark that, for the following results, the stripmap

data has been filtered in order to lower the resolution to the one of the TOPS data.

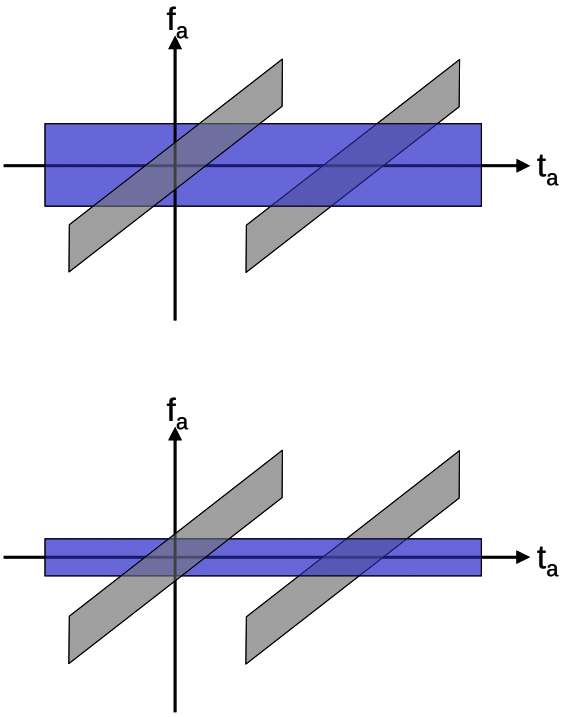

Figure 6. Time frequency diagram for TOPS and stripmap focused signals shown together for comparison. The axis correspond to azimuth time (t_a) and azimuth frequency (f_a). Two contiguous TOPS burst are shown (grey stripes). Note the larger extension of the TOPS signal in frequency domain at burst edges. In that region no azimuth spectral correlation exists with the stripmap signal. (Up) Full resolution stripmap, (down) low resolution stripmap filtered on the TOPS resolution.

Fig. 8 represents the interferometric phase related to the burst in the case of a TOPS slave (up) and a stripmap slave image (down). In the second case, as one can observe, the phase is completely noisy except for the narrow strip in the middle. Therefore the cross interferogram will result in total decorrelation at burst edges and the retrieval of a 2D unwrapped phase with standard procedures is unfeasible. For this reason the DInSAR processing procedure, depicted in Fig. 1, has been slightly modified as shown by the red rectangle on the flow chart of Fig. 9. In particular, the TOPS image acquired on the September 20th 2009 is considered always as master and the interferograms are generated with the remaining TOPS and stripmap acquisitions. Furthermore, assuming a linear deformation trend, it is possible to generate a synthetic deformation phase pattern, for each acquisition date, using the mean deformation velocity estimated in one dataset (the stripmap dataset in the present case). These synthetic deformation phases are then subtracted to each corresponding interferogram. The deviations from the linear trend are supposed to be very small.
Consequently, the residual phases have variations smaller than 2π and can be easily retrieved without unwrapping procedures. Finally, the synthetic phases are again added to these retrieved phases so that, after calibration, it is possible to obtain the deformation maps. These maps track the subsidence movement with a temporal sampling of 11 days.

Fig. 10 shows two examples of deformation estimation performed on CS using the above described procedure. As we can see, the deformation trend estimated by means of cross-interferograms (black stars) is consistent with the ones estimated for TOPS (red diamonds) and stripmap (green triangles), independently. Moreover, it worth noticing that both CS of Fig. 10 are located at the burst edges. This fact demonstrates that the phase of a CS is still preserved despite the lack of azimuth spectral overlap, hence confirming its point-like scatterer characteristic. However, as shown in Fig. 11, estimation errors can occur mainly due to phase retrieval errors, caused by uncorrected atmospheric phase screen contributions.

4. CONCLUSIONS

In this paper we have analyzed a stack of 8 TOPS and 8 stripmap images in terms of time-series performance for subsidence estimation. The estimated deformation using the SBAS technique, which takes into account possible DEM errors and the APS, have shown a good agreement between the TOPS and stripmap results. However, the interferometric processing chain, especially in terms of coregistration accuracy, has to be implemented very accurately due to the TOPS signal characteristics. In any case, it is worth noting that, with respect to the obtained deformation maps, no phase artifacts have been observed at burst edges, hence validating the whole interferometric processing.

The investigation of the deformation using TOPS-stripmap cross-interferograms has been also performed and successfully exploited by means of CS. The results yield that, as expected, the phase is preserved for CS even if there is no spectral overlap. In this study the detection has been performed by means of the CS technique but a detection based on the amplitude stability, as it is done with permanent scatterers (PS), would most probably yield similar results, but a larger stack of images would be required in that case. Due to the decorrelation of distributed targets, the use of interferometric coherence-based DInSAR approaches with cross-interferograms seems not feasible. Moreover,

the processing chain did not consider DEM errors nor APS and has only been done by filtering the stripmap data on the TOPS resolution.

Finally, the results are very satisfactory and neither limitations or restrictions have been found when working with TOPS data, fact that has encouraging implications concerning the ESA's S-1 satellite. Moreover, the possibility to have two satellites like S-1a and S-1b will be a step forward in the reduction of the time between observations facilitating all aspects of interferometric time series processing.

5. REFERENCES

[1] A. Ferretti, C. Prati, and F. Rocca, *"Permanent scatterers in SAR interferometry"*, IEEE Trans. Geosci. Remote Sens., vol. 39, no. 1, pp. 8–30, Jan. 2001.

[2] A. Ferretti, C. Prati, and F. Rocca, *"Nonlinear subsidence rate estimation using permanent scatterers in differential SAR interferometry"*, IEEE Trans. Geosci. Remote Sens., vol. 38, no. 5, pp. 2202–2212, Sep. 2000.

[3] P. Berardino, G. Fornaro, R. Lanari, and E. Sansosti, *"A new algorithm for surface deformation monitoring based on small baseline differential SAR interferograms"*, IEEE Trans. Geosci. Remote Sens., vol. 40, no. 11, pp. 2375–2383, Nov. 2002.

[4] F. De Zan, A. Monti Guarnieri, *"TOPSAR: Terrain Observation by Progressive Scans"*, IEEE Trans. Geosci. Remote Sens., vol. 44, no. 9, pp. 2352–2360, Sep. 2006.

[5] P. Prats, L. Marotti, S. Wollstadt, R. Scheiber, *"Investigations on TOPS interferometry with TerraSAR-X"*, Proce. IGARSS Inter. Geosci. and Remot. Sensi. Sympo., pp. 2629–2632, Jul. 31-Aug. 4 2006.

[6] R. Zandoná Schneider, K. P. Papathanassiou, I. Hajnsek, and A. Moreira, *"Polarimetric and Interferometric Characterization of Coherent Scatterers in Urban Areas"*, IEEE TGRS, vol. 44, no. 4, pp. 971–983, Apr. 2006.

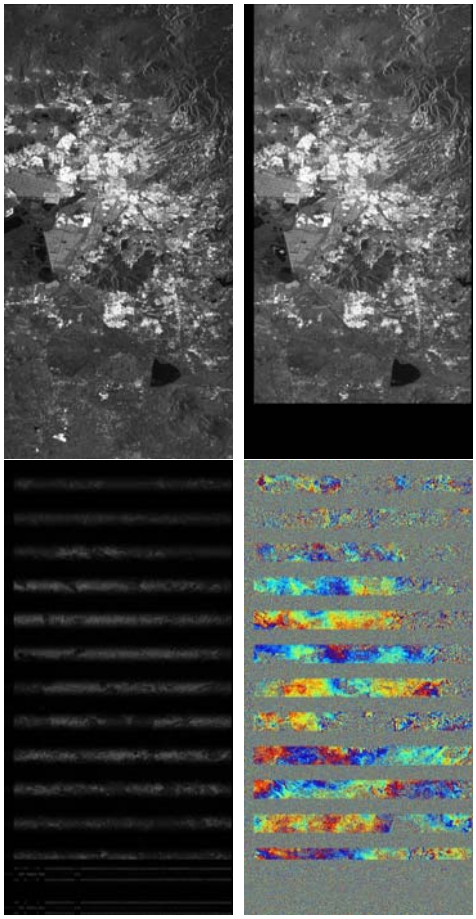

Figure 7. Cross-interferogram between TOPS and full resolution stripmap. The pictures shown are the TOPS reflectivity image (up left), the stripmap reflectivity image (up right), the interferometric coherence (down left), and the flattened interferometric phase (down right), respectively. Coherence estimation window: 17 x 36 (range x azimuth).

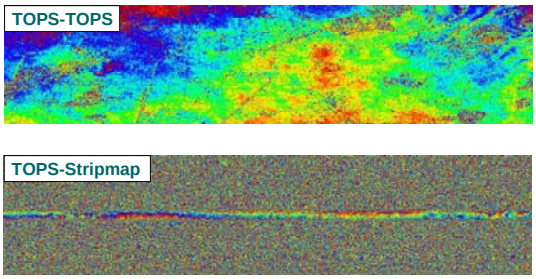

Figure 8. Interferometric phase of one TOPS burst generated by the combination of two TOPS images (up) and a TOPS and a stripmap image (down).

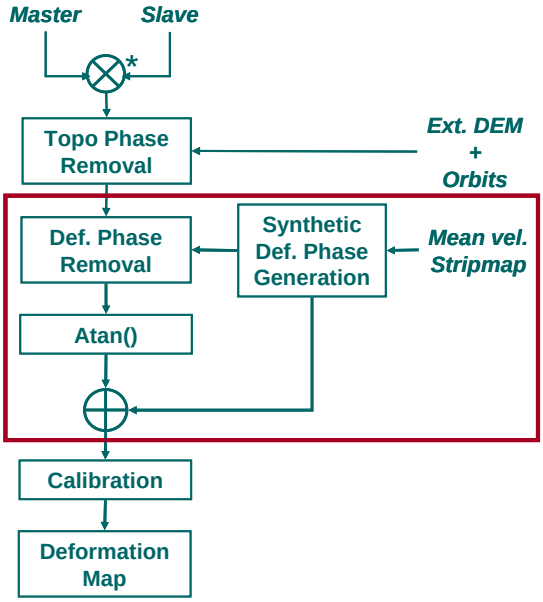

Figure 9. Modified DInSAR flow chart for TOPS-stripmap cross interferograms. The modification is indicated with a red rectangle.

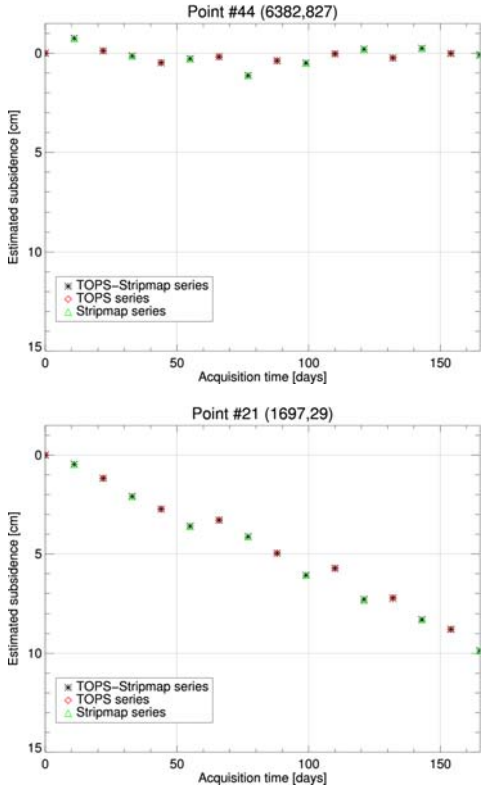

Figure 10. Estimated deformation trend for two CS by means of TOPS data (red diamonds), stripmap data (green triangles) and TOPS-stripmap combination (black stars). Both CS lay at the burst edge (positions 827 and 29, respectively, with a total burst size of 922 samples).

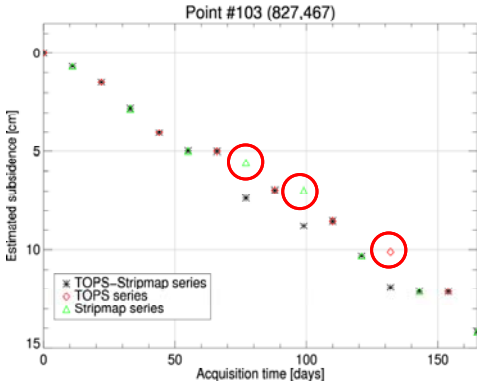

Figure 11. Deformation estimation errors due to wrong phase retrieval.